

## Heatsink Design of High Power Converter

金 燦 起\*  
(Chan-Ki Kim)

**Abstract**—Various ways of designing heat sink are available for commercial high power converters and among them, the method of air cooling is the most popular and practical method than any other ones. In this paper, a practical method of cooling high power converter, which includes a method of reducing noise and vibration caused by the fan and a method of estimating the gap and contact resistances existing between the thyristor and heat sink, is presented. Finally, the heat transfer analysis and implementation methods of heat sink for high power converter is presented.

**Keywords :** Heatsink, Contact and Gap Resistance, Air-Forced Cooling

### NOMENCLATURE

- $T_J$  = Thyristor center temperature,
- $T_{JMAX}$  = Max. temp. of thyristor center,
- $T_C$  = Thyristor case temperature,
- $T_A$  = Air temperature,
- $Q$  = Heat generation rate,
- $R_t$  = Total resistance of heat sink,
- $R_{JA}$  = Overall thermal resistance,
- $R_{JC}$  = Thyristor resistance from junction to case,
- $R_{CS}$  = Resistance from case to surface,
- $R_{csc}$  = Contact resistance between thyristor and aluminum block fin,
- $R_{csg}$  = Gap resistance between thyristor and aluminum block fin,
- $R_{css}$  = Fin conduction resistance,
- $R_{SA}$  = Convection resistance,
- $V_T$  = Max.on-state voltage of thyristor at given on-state current,
- $I_T$  = On-state average current of thyristor,
- $P_{LOSS}$  = Total loss of thyristor.

### 1. INTRODUCTION

Power electronic equipment relies its performance

on the flow control of the electrical current in performing its task. Whenever the electrical current flows through electronic component parts, heat is generated in electronic components such as resistors, diodes, thyristors and transformers.

Fig. 1 shows the converter excitation system, which includes thyristors, field breaker and crowbar circuit. The fundamental principle of heat transfer is that the heat flows from the hot spot to the cool area. Since the electronic components will be usually the hottest spots in the electronic equipment, the heat generated internally, is removed by providing a good heat flow path from the heat sources to an ultimate sink, which is often the surrounding ambient air.

There are three basic methods by which heat can be transferred: **radiation, conduction, and convection**. Most electronic systems make use of all three modes of heat transfer to some extent, while in some cases, they rely largely on one particular mode of heat transfer in the design, such as the case when the greatest amount of heat is picked up by convection

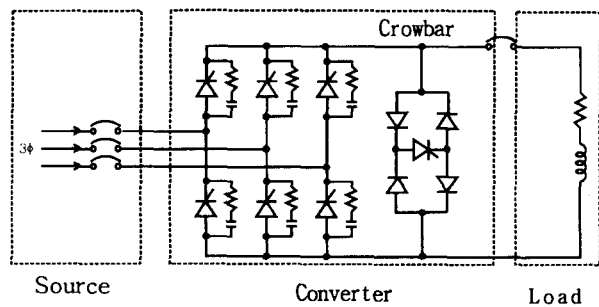


Fig. 1. Diagram of High Power Converter.

\* 正 會 員 : 中央大 電氣科 卒業 · 工博  
接受日字 : 1998년 11월 25일  
最終完了 : 1999년 2월 20일

as cooled air passes over the individual electronic component. Among these modes, heat is transferred by mixing of fluids. When the mixing is due to entirely temperature differences within the fluids, resulting in different densities, the fluid behavior is known as **natural convection**. When the mixing is produced by mechanical means, such as a fan, the action is known as **forced convection**. Natural convection is, in general, much less efficient than the forced convection, because the quantity of cool air flowing in contact with the surface of the heat sink is reduced, and with natural circulation the air local to the fin surface tends to remain stationary or moves very slowly. Considering that most converter systems have many flow blockages which include bus-bar, snubbers and heat sink supporters in the flow path, these blockages can reduce overall cooling efficiency, resulting in surface contamination of the insulator and the heat sink surfaces, which can reduce cooling efficiency. Thus, among forced air cooling products, duct-typed heat sink can be much more efficient than fin-typed one[1].

This paper deals with practical methods of cooling which include the method of reducing noise and vibration caused by the fan and the method of estimating the gap and contact resistance between the thyristor and the heat sink, which was developed for micro-electronics cooling[2]~[6].

## 2. HEAT SINK MODELLING OF HIGH POWER CONVERTER

A thyristor will only function correctly, ie., the block forward and reverse voltage and be controllable by the gate current, if its junction temperature is kept below a critical level. Above this temperature the thyristor cannot be controlled by gate firing and it will not accept the forward voltage without breaking over. This critical junction temperature ranges usually between 120°C and 150°C. The heat dissipated in the vicinity of a junction flows to the case and then to the ambient through the externally mounted heat sink, causing a temperature rise in the junction. The maximum junction temperature of a device should be limited because of its adverse effect on the leakage current, breakover, turn-off time, thermal stability, and long-term reliability of the device.

Fig. 2 shows the thermal equivalent circuit of a thyristor mounted on a heat sink. During steady state, the thermal capacity may be ignored but

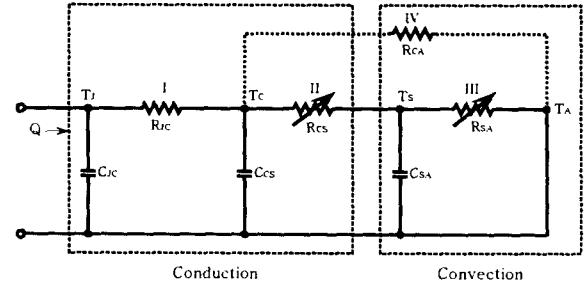


Fig. 2. Thermal equivalent circuit of a thyristor mounted on a heat sink.

during the transient state or heat sink test it must not be neglected. In Fig. 2, the thermal resistance  $R_{CA}$ , which is the resistance between the case and ambient air, was deleted in the present analysis because its value is negligible compared to other resistance values. For sustained power dissipation  $Q$  at the junction, the steady-state junction temperature  $T_J$  can be calculated as:

$$T_J = Q(R_{JC} + R_{CS} + R_{SA}) + T_A \quad (1)$$

$$R_{JC} = \frac{L_1}{h_{JC}A_{JC}} \quad (2)$$

$$R_{CS} = \frac{L_2}{h_{CS}A_{CS}} \quad (3)$$

$$R_{SA} = \frac{1}{h_{SA}A_{SA}} \quad (4)$$

In Equations (1), (2), (3) and (4),  $A_{JC}$ ,  $A_{CS}$  and  $A_{SA}$  represent the contact surfaces from junction to case, case to heat sink and sink to ambient respectively.  $L_1$  and  $L_2$ , represent the thickness from junction to case and case to heat sink. The variable  $h_{SA}$  is the coefficient of convection heat transfer,  $h_{JC}$  is the thermal conductivity coefficient from junction to case, and  $h_{CS}$  from case to heat sink. From Equation (1) it is evident that for a limited  $T_{JMAX}$ , the heat flow rate  $Q$  can be increased by reducing  $R_{SA}$ . This means that more efficient cooling system will enhance the device capability of power dissipation. An infinite heat sink will be resulted if

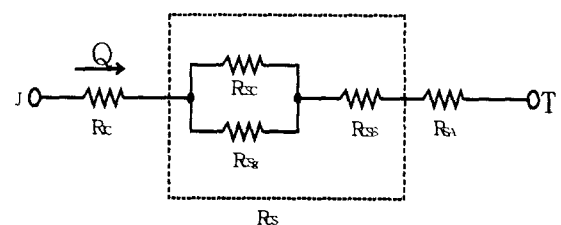


Fig. 3. Detailed thermal circuit for thyristor cooling.

$R_{CS}$  and  $R_{SA}$  are reduced to zero and the case temperature,  $T_C$  is limited to the fixed ambient temperature  $T_A$ . Figure 3 shows a detailed thermal circuit for thyristor cooling.

In Fig. 3, the resistance  $R_{CS}$  is a complex summation of surface and interstitial(gap) resistance, known as the mounting or interface thermal resistance. The gap at the interface is caused by the uneven surfaces being joined together and resultant air gap generates additional thermal resistance that can be reduced through the use of special compounds designed for industry application. Thermal resistance,  $R_{CS}$  may also include the overall resistance of insulators placed between the case and heat sink;  $R_{CS}$  may be minimized by following strict assembly procedures. Mounting force, which is relation to  $R_{CS}$  shown in Figure 2 and Equation (3), are necessary to establish a good electrical and thermal contact. It is very important that the mounting force stays within design specification even under the worst condition, ie. over the whole operating temperature range. Too low mounting force results in an increase in thermal resistance and, particularly with high currents, damage of the dry interfaces within the housing and possible degradation of the device. Exceeding mounting force over design specification leads to an increased mechanical stress on the silicon wafer, particularly in applications with frequent thermal cycles. This reduces the life expectancy of the device and can lead to premature wear-out. The variable for the designer is the thermal resistance from heat sink to ambient,  $R_{SA}$ . Controlling  $R_{SA}$  with fixed  $Q$  determines the amount of sink temperature rise above ambient air temperature in the heat path. It can shift all the other temperature up or down. Changing  $R_{SA}$  also varies the overall thermal resistance  $R_{JA}$ , which, in turn determines to what extent the input power  $Q$  could be increased while not exceeding the specified junction temperature  $T_J$ . From Figure 3, the performance of an air-cooled heat sink will depend on followings factors:

- (1) Surface area exposed to the cooling air.
- (2) Heat sink efficiency in transferring heat from the thyristor to the dissipating surface.
- (3) Heat sink material.
- (4) Size of the thyristor surface in contact with the heat sink.
- (5) Position of the thyristor on the heat sink.
- (6) Ambient air temperature.

- (7) Volumetric flow of air over the fin surface.
- (8) Nature of the air flow, ie. laminar or turbulent flow.
- (9) Mounting force between the thyristor and the heat sink.
- (10) Surface roughness between the thyristor and the heat sink.

Among above factors, the most efficient cooling factor is thyristor current capability, the surface exposed to the cooling air and the air flow rate. When designing a large converter, it is necessary to select the thyristor before deciding the size of the radiative plate with fins because large capacity radiative plate is not popular like small scale ones. Generally, selection of the thyristor is made considering normal current, surge current ratio and thermal resistance. When the allowance of the normal current for the thyristor is increased, it can endure thermal aging and heat is less dissipated from the thyristor. This enables to have small radiative plate and as the allowance gets smaller, it should have larger radiative plate. The current radiative plate was manufactured in a aluminum duct shape with fixed length(L), height(H), and cuttable width(W) as desired. Since the cooling fans consume electricity and have possibility of failure due to noise and vibration, the procedure for the design of high power converter is to select thyristor, design the radiative plate and then the capacity of the cooling fan.

### 3. HEAT SINK DESIGN OF HIGH POWER CONVERTER

The high power converter is designed with the assumption that it shall be operated at the ambient temperature of 25°C in normal use and 50°C in harsh conditions. The maximum temperature of the thyristor junction is limited to 70°C that is lower than the usual limiting temperature of 90°C because the thyristor may be damaged by instantaneous heat caused by the peak voltages or currents. The heat generating thyristor is mounted to the rectangular aluminum fin block(duct-typed block). Since DC current of present application is 1000[A], a selected thyristor is ABB Model Number 5STP 45N2800. Considering the size of the converter system and life expectancy of thyristor, an thyristor is selected. In general, if the thyristor current capability is large, the life of the thyristor aging will enlarge because  $di/dt$  and  $dv/dt$  rate of the thyristor decrease[7].

### 3.1 Heat Generation Rate From the Thyristor[8],[9]

Since the DC output current(  $I_{DC}$  ) of the converter is  $I_T$ , the average current of the three phase converter can be estimated by

$$I_T = I_{DC}/3 \quad (5)$$

Using Equation (5), total power loss can be calculated as follows :

a) On-state power loss(  $P_{ON-LOSS}$  )

$$P_{ON-LOSS} = \frac{I_T(V_T + RI_T(\frac{2\pi - \mu}{2\pi}))}{3} \quad (6)$$

where, R is a thyristor differential resistance and  $\mu$  is a overlap angle in radians.

b) Turn-on Power Loss(  $P_{SON}$  )

$$P_{SON} = F_{GVI} \times \text{Frequency} \quad (7)$$

where  $F_{GVI}$  is the factor for forward gate voltage vs. forward gate current.

c) Turn-off Power Loss(  $P_{SOFF}$  )

$$P_{SOFF} = F_{RC} \times \text{Frequency or} \\ = \sqrt{2}V_L Q_r f \sin(\alpha + \mu + 2\pi\sqrt{\frac{Q_r}{di/dt}}) \quad (8)$$

where,  $F_{RC}$  is the factor for turn-off energy-per-pulse vs. quasi-static reverse voltage at  $di/dt$ ,  $V_L$  is a line-to-line commutating voltage,  $Q_r$  is a average value of charge stored at thyristor in Coulombs and  $di/dt$  is a rate of change of current at  $I=0$  in amperes/second.

Therefore, the total power loss is the sum of on-state power loss, turn-on power loss and turn-off power loss. The total loss becomes following as :

$$P_{LOSS} = P_{ON-LOSS} + P_{SON} + P_{SOFF} \quad (9)$$

### 3.2 Overall Heat Transfer Calculation

If one knows the heat generation rate from the thyristor and the temperature of air, one can estimated the limiting temperature of the thyristor. The total resistance involved in the thermal circuit is as follows

$$R_t = R_{JC} + \frac{1}{\frac{1}{R_{csg}} + \frac{1}{R_{csc}}} + R_{css} + R_{SA} \quad (10)$$

Since the total heat transfer rate is expressed as

$$Q_{th} = \frac{T_J - T_A}{R_t} \quad (11)$$

The junction temperature of the thyristor  $T_J$  is expressed as

$$T_J = Q_{th}R_t + T_A \quad (12)$$

### 3.3 Thyristor Resistance( $R_{JC}$ ) Calculation

Since it is difficult to evaluate the effective thermal conductivity of thyristor with different layers, measurements of effective thermal conductivity of thyristor was conducted as shown in Fig. 4.

The experimental apparatus consists of the test chamber, loading mechanism and data collection system as shown in Fig. 5.

From the top of the test column, there are heater block, upper heat meter, thyristor and lower heat meter coaxially in order to take an average heat flux value with cylindrical brass heater block containing two 100W pencil type electrical heaters. A 300mm diameter cold plate supports the lower heat meter

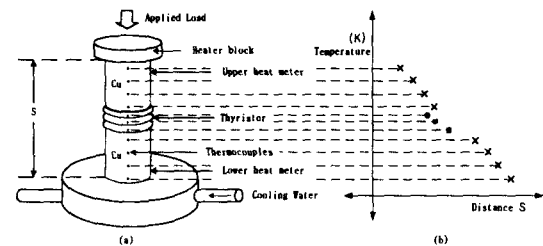


Fig. 4. Thermal resistance measurement for thyristor

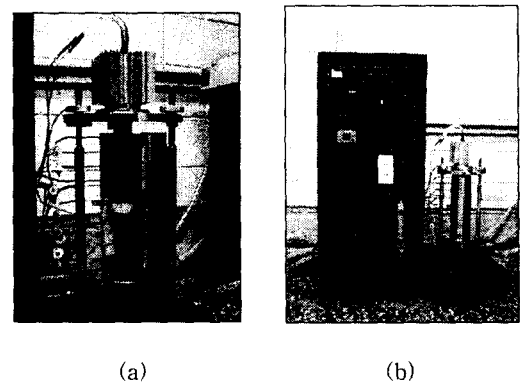


Fig. 5. Experimental test rig to measure thermal junction resistance

coaxially. A mechanical load up to 200kN could be axially applied to the test column by means of diaphragm-type air cylinder. Four J-type thermocouples for each meter, and three thermocouples for the thyristor were embedded in drilled holes with epoxy to measure the temperature gradients with measured heat flow rate.

### 3.4 Joint Thermal Conductances

The joint thermal conductances at the interface  $h_j$  can be expressed as the sum of contact conductances  $h_c$  and gap conductances  $h_g$ , which can be expressed as

$$h_j = h_c + h_g \quad (13)$$

Two different thermal contact resistances exist in the analysis. One is the joint resistance between positive(+) and negative(-) diode layers inside the thyristor(called junction to case) and the other is between bottom surface and the aluminum fin base surface(called case to heat sink). The theoretical thermal contact conductances models or correlations for heat transfer across interfaces formed by contacting metallic isotropic surfaces were developed by Cooper, Mikic and Yovanovich[2] and Yovanovich[3]. Recently, De Vaal, Yovanovich and Negus[4]~[6] developed a thermo-mechanical model to take contact orientation into account for anisotropy surface pairs. The contact conductances correlation developed for isotropic surfaces is summarized as below[3].

$$h_c = 1.25 \left( \frac{m}{\sigma} \right) k_s (P/H_c)^{0.95} \quad (14)$$

with a maximum error less than  $\pm 1.5\%$  for  $10^{-6} \leq P/H_c \leq 2.3 \times 2.3 \times 10^{-3}$  where  $P$  is the apparent contact pressure,  $H_c$  is the contact microhardness,  $m/\sigma$  is the effective interface surface roughness parameter,  $k_s$  is the harmonic thermal conductivity.

The effective surface roughness  $\sigma$  and the mean absolute surface slope are defined as

$$\sigma^2 = \sigma_A^2 + \sigma_B^2 \quad (15)$$

$$m^2 = m_A^2 + m_B^2 \quad (16)$$

where  $\sigma_A, \sigma_B, m_A$  and  $m_B$  are obtained from the surface profile measurements on each surface.

Song and Yovanovich[5] developed an explicit expression for the relative contact pressure for a

given contact pressure and surface parameters.

$$\frac{P}{H_c} = \left[ \frac{P}{C_1} (1.62\sigma/m)^{C_2} \right]^{\frac{1}{1+0.071C_2}} \quad (17)$$

where  $C_1$  and  $C_2$  are the Vickers correlation coefficients. This correlation has a maximum error less than  $\pm 2\%$  for  $10^{-6} \leq P/H_c \leq 2.3 \times 10^{-2}$ .

Since the surfaces of selected thyristor (ABB Model Number 5STP 45N2800) are lapped on both sides(Material A) and the surface of aluminum heat sink(Material B) are lapped, the following data were used for surface parameters, which were obtained from the surface profile measurements[8] as listed in Table 1. The thermal conductivities of both materials were obtained from [1].

As shown in Table 1, the surface roughnesses of radiative plate and thyristor can affect the thermal resistance. Present analysis uses surface roughness value obtained by milling. The harmonic mean thermal conductivity,  $k_s$  is calculated from

$$k_s = \frac{2k_A k_B}{k_A + k_B} \quad (18)$$

**Table 1.** Thermophysical Parameters and Surface Roughness Parameters.

Material	Thyristor(A)	Rectangular Fin Surface(B)
Surface Roughness, $\sigma$ ( $\mu\text{m}$ )	0.1	0.15
Mean Slope, $m$	0.01	0.02
$m/\sigma$ ( $\mu\text{m}^{-1}$ )	0.1	0.13
Thermal Conductivity (W/mK) at 300K	148 (silicone)[1]	237 (pure aluminum)[1]

**Table 2.** Thermochemical Properties of Air used in the Calculation [1].

Thermochemical Properties	Used Values
Thermal conductivity $k_{go}$ (W/mK)	$2.624 \times 10^{-2}$
Thermal accommodation coefficient $\alpha$	0.6
Density, $\rho$ kg/m <sup>3</sup>	1.1769
Viscosity, Pa · s	$1.8464 \times 10^{-5}$
Ratio of specific heats $\gamma$	1.5
Prandtl number Pr	0.708
Molecular mean-free-path $\lambda$ ( $\mu\text{m}$ )	0.1

The gap conductances  $h_g$  is the conductances through the gas filled in the gap between two materials and it can be calculated from [3]

$$h_g = \frac{k_{go}}{(Y+M)} \quad (19)$$

where  $k_{go}$  is gas mean thermal conductivity,  $Y$  is mean plane separation between the two surfaces.

$$Y = 1.184\sigma[-\ln(3.132P/H_c)]^{0.547} \quad (20)$$

and  $M$  is gas parameter

$$M = \alpha\beta\lambda = \left(\frac{2-\alpha_1}{\alpha_1} + \frac{2-\alpha_2}{\alpha_2}\right) \left(\frac{2\gamma}{\gamma} + 1\right) \frac{1}{Pr} \lambda \quad (21)$$

where  $\alpha$  is thermal accommodation coefficient,  $\beta$  is  $2\gamma/(\gamma + 1)$ ,  $\gamma$  is the ratio of specific heats,  $C_p/C_v$ ,  $\lambda$  is molecular mean-free-path ( $\mu\text{m}$ ), and  $Pr$  is Prandtl number.

For air gap between the thyristor and aluminum heat sink, the following physical properties were used. This thermal resistance exists between the thyristor bottom surface and the aluminum heat sink when there is an air gap and with the bolted joint force of 90kN.

### 3.5 Conduction Shape Factor

The thermal resistance  $R_{css}$  for steady two and three dimensional conduction heat transfer is defined as

$$R_{css} = \frac{1}{kS} \quad (22)$$

where  $S$  is the conduction shape factor for particular geometry of the fin,  $k$  is the thermal conductivity.

For the geometry of thyristor and rectangular the aluminum fin with heat dissipation at the center, the following equation was used to estimate the conduction shape factor,  $S$ [6]

$$S = \frac{2\pi L}{\ln(1.08W/D)} \quad (23)$$

where  $L$  is the fin base thickness,  $D$  is the diameter of region with higher temperature,  $W$  is the width of the fin geometry.

### 3.6 Convection Coefficient

For a rectangular block of the fin, the hydraulic diameter is calculated as [6]

$$D_h = \frac{4A_c}{P_c} \quad (24)$$

where  $P_c$  is the perimeter of a fin,  $A_c$  is the cross section of the fin hole.

Then, the air mass flow rate for a fin hole is calculated as

$$m = \rho V \quad (25)$$

The Reynolds number is calculated as

$$Re_D = \frac{4m}{\pi D_h \mu} \quad (26)$$

This range of Reynolds number is in turbulent flow. For fully-developed turbulent flow in a smooth circular tube, Dittus-Boelter equation was used[6].

$$Nu_D = 0.023 Re_D^{4/5} Pr^{0.3} \quad (27)$$

this correlation was experimentally confirmed for the range of conditions as

$$0.7 \leq Pr \leq 160, Re_D \geq 10,000 \text{ and } L/D \geq 10 \quad (28)$$

The thermal resistance due to heat convection by air blow is

$$R_{SA} = \frac{1}{h_{SA} A_{SA}} \quad (29)$$

Consequently, Fig. 6 shows the design elemental geometry of rectangular fin and thyristor. And Table 3 shows the summary of thermal resistance for half fin with  $W=300\text{mm}$  involved in the thermal circuit.

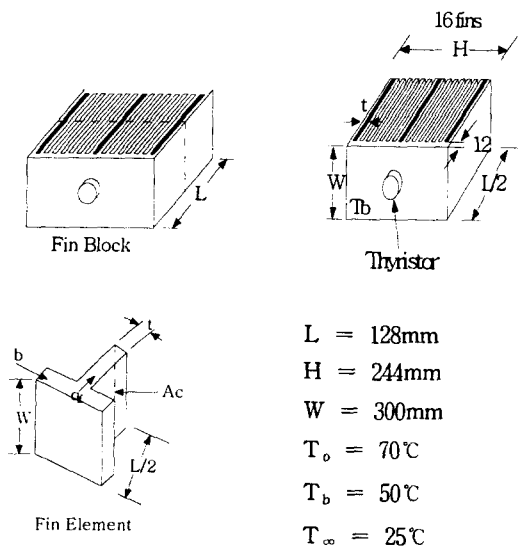


Fig. 6. Elemental geometry of rectangular fin and thyristor.

**Table 3.** Thermal Resistances Involved in half fin with W=300mm.

Contact Resistance R <sub>CSC</sub> (K/W)	Gap Resistance R <sub>CSG</sub> (K/W)	Convection Resistance R <sub>SA</sub> (K/W)	Conduction Resistance R <sub>CSS</sub> (K/W)
9.6 × 10 <sup>-3</sup>	6.7 × 10 <sup>-3</sup>	4.9 × 10 <sup>-3</sup>	7.2 × 10 <sup>-3</sup>

### 4. STRUCTURE OF HIGH POWER CONVERTER

#### 4.1 Noise and Vibration Reduction of High Power Converter

Noise Vibration Frequency(NVF) generated in the heat sink by a fan is represented as follows:

$$NVF = \frac{S}{60} * P \tag{30}$$

where, P is the number and S is the rotating frequency of fan. Also, RF(Resonant Frequency) of mechanical system is represented as :

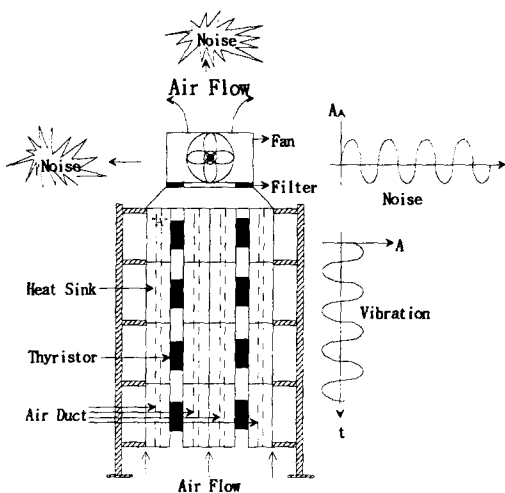


**Fig. 7.** Heat sink construction.

$$RF = \frac{1}{2\pi} \sqrt{\frac{nk}{m}} \tag{31}$$

To solve this problem, a mechanical filter(spring) was inserted between the fan and heat sink. Spring elasticity coefficient between the fan and the system can be designed by avoiding the value of Equation (32), where n is the elasticity coefficient between the fan and heat sink, k is mechanical filter numbers and m is fan mass. In this system, if the resonant frequency of the fan is the same as the mechanical resonant frequency of this system shown as Equation (31), this system will produce a noise and vibration.

$$\frac{S}{60} * P = \frac{1}{2\pi} \sqrt{\frac{nk}{m}}$$

$$n = \frac{(2 * P * S * \pi)^2 * m}{3600 * k} \tag{32}$$

#### 4.2 Construction of High Power Converter

In general, thyristor assembly construction is guided by the following points:

- (1) Electrical and thermal contacts are usually at the same points.  
(Electrical connection is taken from the heat sink. The heat sinks will be at different potentials.)
- (2) The necessity to incorporate heat sink into the overall cooling circuit causes thyristors to be installed inside the assembly, particularly with double-sided cooling, making accessibility more difficult.
- (3) The thyristors need to be surrounded by surge suppression, and snubber circuits
- (4) The thyristors, diodes, commutating capacitors, and inductors in forced- commutated circuits may need to be mounted in very close proximity to each other to avoid stray circuit inductances.
- (5) Construction in the form of removable sub-assemblies can considerably help for the maintenance of the equipment when in service.

### 5. ANALYSIS AND DESIGN OF HEAT SINK

Fig. 8 shows calculation results for the heat sink with a fan by the commercially available heat transfer code FLUENT, as seen in previous Fig. 7.

Fig. 8(a) displays the heat distribution of the heat sink, and Fig. 8(b) the distribution of heat flow.

Fig. 9, showing the heat sink with blockage,

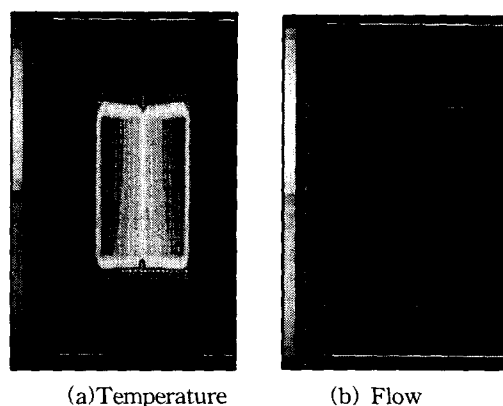


**Fig. 8.** Heat dissipation of heat sink

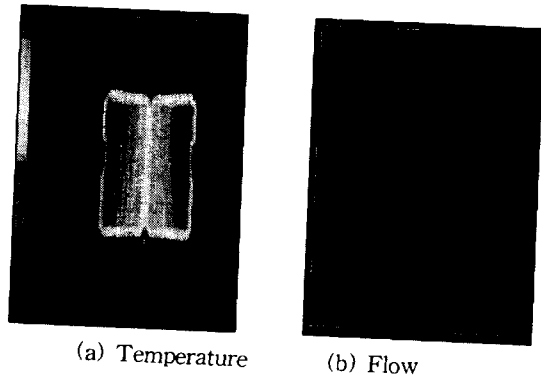


Fig. 9. Heat dissipation of heat sink with blockage

shows a slight increase in its temperature since the heatsink was designed to have a duct for heat flow.

Also, in order to utilize a buoyant effect in heat transfer, a resistance component was installed on an upper heat sink part, whose heat distribution is displayed in Fig. 10 considering other heat element. An experimental test rig to measure the thermal resistances is shown in Fig. 11. The fan shown in Fig. 11(d) was designed for emergency backups.

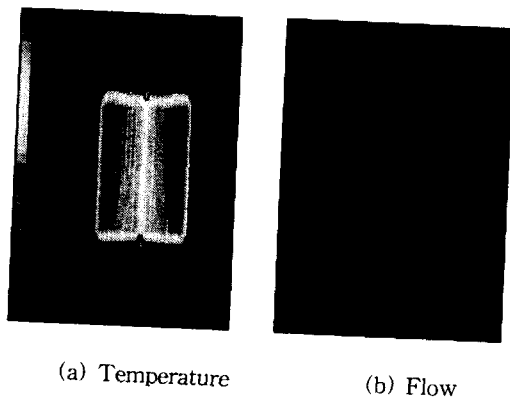
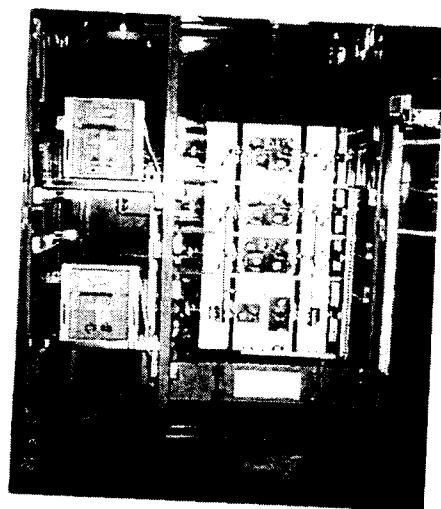
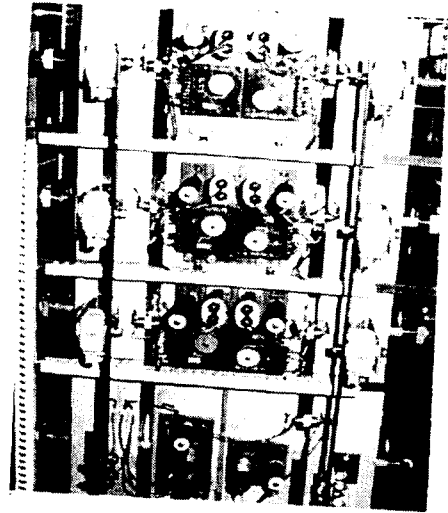


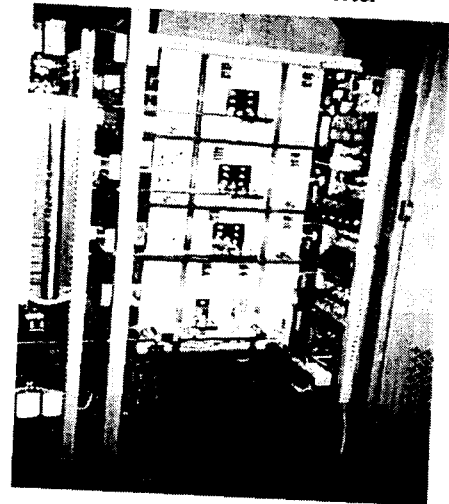
Fig. 10. Heat dissipation of heat sink



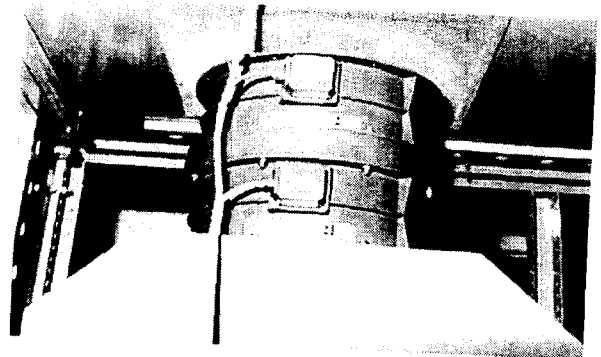
a) Overall Configuration of the converter



b) Front of the converter



c) Back of the converter



d) Fan of the converter

Fig. 11. Implemented heat sink of high power converter.

## 6. CONCLUSION

An efficient heat sink system is presented in this paper, which can replace the conventional heat sink system with additional features such as considering more advanced heat transfer analyses and reduction



of noise and vibration caused by fans. The proposed method in this paper can be applied to IGBT, GTO converter.

### REFERENCE

- [1] A. F. Mills, "Heat Transfer", Richard D. IRWIN, INC., 1992.
- [2] Cooper, M.G., Mikic, B.B. and Yovanovich, M.M., "Thermal Contact Conductances", International Journal of Heat and Mass Transfer, Vol.12, 1969, pp. 279-300.
- [3] Yovanovich, M.M., "Thermal Contact Correlations", "Spacecraft Radiative Transfer and Temperature Control" Edited by T.E. Horton, Vol. 83 of Progress in Astronautics and Aeronautics, New York, 1982.
- [4] De Vaal, J.W., Yovanovich, M.M. and Negus, K.J., "The Effect of Surface Slope Anisotropy on the Contact Conductances of Conforming Rough Surfaces", "Fundamentals of Conduction and Recent Development in Contact Resistance, ASME HTD-Vol. 69, pp.123-134., 1987.
- [5] Song, S and Yovanovich, M.M., "Relative Contact Pressure Dependence on Surface Roughness and Vickers Microhardness", AIAA Journal of Thermophysics and Heat Transfer, Vol. 2, No.1, pp.43-47, 1988.
- [6] Yovanovich, M. M., Culham, J. R. and Teertatra, "Calculation interface resistance", Electronics Cooling, Vol. 3, No. 2, May 1997, pp. 24-pp.29.
- [7] Yoshio Shimoda and Hidetaka Satoh, "Waveform dependence of Surge-handling Capability and Failure Analysis for Semiconductor Lighting Surge Protectors", Japan Journal of Application of Physics, Vol. 34, pp. 5993~pp.5997, 1995.
- [8] "IEEE Recommended Practice for Determination of Power Losses in HVDC Converter Station", IEEE Standard 1158-1991.
- [9] Peter Lips, "Loss Calculation of HVDC Thyristor Valve", IEEE Transactions on Power Delivery, Vol. 3 No. 1, Jan. 1988, pp.358-362.
- [10] D. Finney, "The Power Thyristor and its Applications", McGraw-hill, 1980.
- [11] Thyristor Data Book, ABB INC. 1995.
- [12] M. Necati ozisik, "Heat Transfer-a Basic Approach", McGraw-Hill, 1981.
- [13] H.P.Lips, "Water Cooling of HVDC Thyristor valves", IEEE Tran. on Power Delivery, Vol.9, No.4, Oct. 1994, pp.1830~1837.
- [14] P.O. Jackson, etc. 3, "Corrosion in HVDC valve cooling systems", IEEE Tran. on Power Delivery, Vol. 12, No. 2, April, 1997, pp.1049~1052.

## 저 자 소 개



김 찬 기 (金 燦 起)

1968년 12월 17일. 1991년 서울산업대 전기과 졸업. 1993년 중앙대 전기과 졸업(석사). 1996년 중앙대 전기과 졸업(공학). 1996년 전력연구원입사. 송 변전 기술그룹 선임연구원 IEEE 논문심사위원. 1998년 미국 Who's who 인명사전에 등재(예정). 주관심분야 : 전력 변환장치, 전동기 드라이브, HVDC, 현대 제어 이론

Tel : (042) 865-5892  
E-mail : CTkim@kepri.re.kr